

Study of Hydraulic Failure Mechanism in the Core of Eyvashan Earth Dam with the Effect of Pore Water Pressure and Arching

M. Komasi*, B. Beiranvand

Civil Engineering Department, Water and Hydraulic Structures, University of Ayatollah ozma Borujerdi, Lorestan, Iran.

Article info

Article history:

Received 06 September 2019

Received in revised form

06 January 2020

Accepted 09 February 2020

Keywords:

Eyvashan dam

Hydraulic failure

Pore water pressure

Arching

Geostudio

Abstract

Continuous investigation and measurement of pore water pressure and arching depression play an important role in detecting the occurrence of hydraulic failure in earth dams. Increasing the pore water pressure during the initial impounding period reduces the effective stress and consequently decreases the shear strength of the earth dam core, which can overcome the water stress over the effective stress and consequently hydraulic failure. This research studies the hydraulic failure of Eyvashan earth dam under static loading conditions at the end of construction and the initial impounding period by Geostudio software with the Mohr-Coulomb behavioral model. The analysis shows that the values of the pore water pressure ratio (r_u) and stress-strain values are acceptable and there is no stability problem for the dam. The highest percentage of arching (the lowest ratio of arching) is equal to 46%, at one-third of the lower height of the core. The critical arching ratio (maximum) is 0.44 and is in the normal range and hydraulic failure does not occur despite the critical arching in the dam core.

1. Introduction

Measuring the pore water pressure to control stability of foundation and body of dams are of particular importance. Moreover, recognition of initial stress and material characteristics plays an important role in recognizing the behavior and realistic modeling of earth dams. In fact, the importance of examining the internal stresses of the earth dams is because the state of the settlement, as well as the core's vulnerability or its sustainability, is a function of these tension distributions. Vertical and horizontal internal stresses at the core of dam should be more hydrostatic pressure. In cases where vertical and horizontal stresses are low, the risk of hydraulic fracture increases. The frictional resistance between the core and the shell causes arching. Due to the fact that the phenomenon of arching

is one of the most important factors in hydraulic fracture and destruction of earth dams and its failure to pay attention to irreversible damages to the dam and stability, so predicting the state of arching is of particular importance. Generally, various parts of dams, due to different characteristics, have different settlements that cause the transfer of stress from the masses with a higher settlement to the lateral hardened masses with less settlement through the adhesion and shear strength. Furthermore, the softer mass relies on the harder adjacent mass. Typically, the back analysis expressed as a way to control the system parameters by analyzing its output behavior. This method has been used in recent years. In the back analysis first, the values of displacement, strain, and, if necessary, the stresses are calculated by the instrument and then replaced in a hypothetical mechanical model; finally, the

*Corresponding author: M. Komasi (Associate Professor)

E-mail address: komasi@abru.ac.ir

<http://dx.doi.org/10.22084/jrstan.2020.20022.1110>

ISSN: 2588-2597

parameters of the initial stress, mechanical properties, and boundary conditions are determined. Hydraulic failure is the process of starting or developing a small physical separation, such as cracking. In rock-fill and earth dams in the initial impounding period, increasing reservoir water pressure causes tensions to approach the upstream of the impermeable core with a shear or tensile mechanism close to the rupture. As a result, cracks may occur in some areas of the upstream core. These cracks are referred to as hydraulic fracturing pressures due to the hydraulic cracks and water pressure required to create them. Löfquist [1] was the first to study arching in the core of dams and study the possibility of horizontal cracks occurring through arching. Sherard [2], with consideration of the angle of expansion as a function of the angle of friction and the Mohr-Coulomb behavioral hydraulic fracture, carried out analyses to determine the force necessary for the occurrence of hydraulic failure. He believed that hydraulic failure occurs at the core when the smaller original stress (σ_3) at a certain height is less than the water pressure at the core at the same height. Maksimovic studied the arching core of dams in a finite element method. In his calculations, he considered the behavior of materials as elastic and the construction of dam single-stage. The assumption of the construction of a single-stage dam and the non-consideration of the plastic behavior of the materials led to an arching value higher than the real value [3]. Additionally, Kulhawy and Gurtowski [4], studied arching and hydraulic failure in dams with a vertex core; it was concluded that the phenomenon of stress transfer in non-homogeneous earth dams occurs due to a change in the adjacent areas. Wang et al. [5], Soga et al. [6], Satoh and Yamaguchi [7], Mansoorjian et al. [8], Molavi and Parvishi [9], Rezapur Tabari and Hashempour [10], Abbasi et al. [11] investigated the hydraulic deflection of dams. Khamesi and Mirghasemi [12] considered the occurrence of hydraulic failure as unlikely due to the study of Golabar dam clay. Moreover, the results of Salari et al. [13] on hydraulic failure in the clay core of dam in the Tang Valley showed that the hydraulic failure phenomenon could be one of the main causes of the internal erosion at the clay core of the Bidwaz dam. Asakareh and Ahang [14] studied the effective parameters in the arching phenomenon in non-homogeneous Baft Dam model by Plaxis software and it was determined that the width of the core, the thickness of the filter layer, and the density of the foundation had the greatest effect on arching the earth dams, respectively. In this research, numerical analysis by Plaxis software was used to study variations in pore water pressure, strain, and bending of Eyvashan earth dam and the possibility or impossibility of hydraulic failure using theoretical analysis and analysis of the results.

2. Materials and Methods

2.1. Eyvashan Earth Dam

Eyvashan Reservoir Dam is located 1.5km from the upstream of the village of Eyvashan and about 57km from Khorramabad in the coordinates of 48°49'2"N and 33°28'31"N, located on the Horod River. The area of the Horod river drainage basin up to the axis of dam of Eyvashan is 120km². The dam is a rock-fill-earth dam type with a vertical clay core that has a height of 62m (1804m above sea level), a crest height of 1868m and a normal elevation of 1864m above sea level. The volume of the reservoir in the normal level of dam is 52 million m³ and the area of the lake at normal level is 2.3km². Fig. 1 presents the Eyvashan earth dam view.



Fig. 1. Eyvashan earth dam.

The construction site of the Eyvashan reservoir from the geological point of view of the rock bed consists of conglomerate rocks that have outcrops in the boundaries of these rocks but deposited on the conglomerate rock in the bottom of the valley of alluvial sedimentary deposits. In terms of lithology, the conglomerate of the axis and lake is composed of limestone, sandstone, slate, metamorphic rocks, and igneous rocky parts with a silty-sandy and sometimes silt-clay matrix.

2.2. Instrumentation Eections of Eyvashan Earth Dam

The instrumentation of the Eyvashan earth dam in four cross-section with numbers 228-228, 229-229, 230-230, and 231-231 is considered in 0+249, 0+356, 0+477, and 0 + 546, respectively. In the present study, the characterization of the instruments installed in the section of 229 Eyvashan earth dams was investigated. In Fig. 2, the position of the cross-sections and the section of the instrumentation 229 of dam is shown. The highest level of instrumentation is related to the 229-229 cross-section with seven levels and the least number of Instrumentation levels is related to the 231-231 section with five levels. Electrical Piezometer Embankment (EPE) and Total Pressure Cell (TPC) piezometers are shown in Fig. 2.

2.3. Investigating the Results of Instrumentation of Pore Water Pressure and Arching of Eyvashan Dam

The pore water pressure in the clay core of the earth dam is very important in terms of soil mechanics and its increase can compromise the stability of dam. When the high water pressure in the body of the earth dam is created, it can reduce the effective stress and thus reduce the shear strength of the core materials and, finally, create cracks or collapse in dam body. Therefore, reducing the excess pore pressure in the body of dam is very important during the construction and operation of dam. Furthermore, the phenomenon of arching is dependent on the difference in shell and core alignment (core consolidation) and the shear strength between the core and the shell of dam. Clay, especially if it is normally consolidated, has a lot of settlements. This settlement in the core causes the difference in the settlement between the core, shell, and filter. The core tends to settlement more (relative to the adjacent hard shell), which, under the weight, results in the transfer of a portion of the core weight to the adjacent hard shell, and its connection to the filter, also, provides a field for the arching phenomenon. As a result, in the core, the vertical stress is less than the overhead and

in the adjacent shell is the opposite. It transfers the weight from the core to shell to arching the core into a shell. By decreasing vertical pressure in the core, damping and reducing the effective stresses, there is the possibility of water penetration, hydraulic failure, and dam destruction. The coefficient and rate of arching of the core is derived from relations 1 and 2 [15]:

$$\text{Arching coefficient} = \frac{\sigma_v}{\gamma \cdot h} \tag{1}$$

$$\text{Arching rate} = (1 - \text{Arching coefficient}) \times 100 \tag{2}$$

where σ_v is the effective vertical stress inside the core, γ is the specific gravity of the core and h is the height of the embankment. The higher the arching coefficient, the lower the arching rate (arching percent) is. Furthermore, the higher the percentage of arching, the more effective the arching can be, and the more stress levels can be reduced. If tensions in the elevation of the dam are reduced by less than water pressure at the same level, it may result in hydraulic fracturing or crack formation due to high water pressure, and then there is a possibility of piping. The hydraulic fracturing pattern due to arching, which engineers often encounter in field conditions at the cross-section of dam, are shown in Fig. 3.

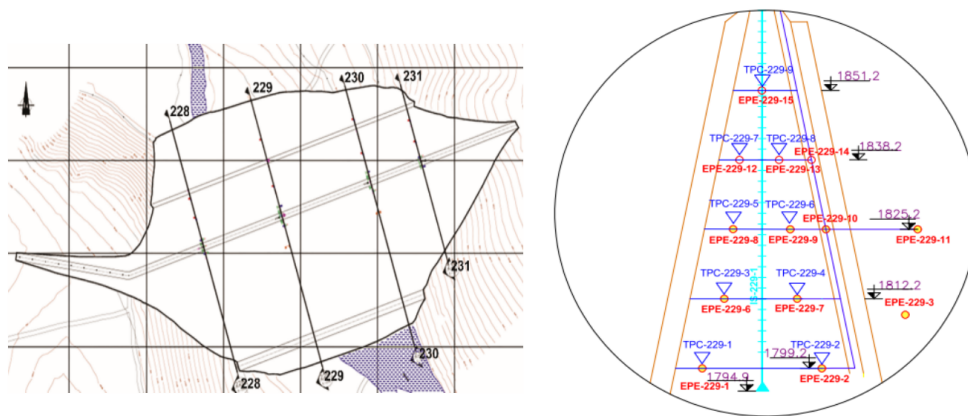


Fig. 2. Position of instruments on the plan and cross-section of the Eyvashan earth dam.

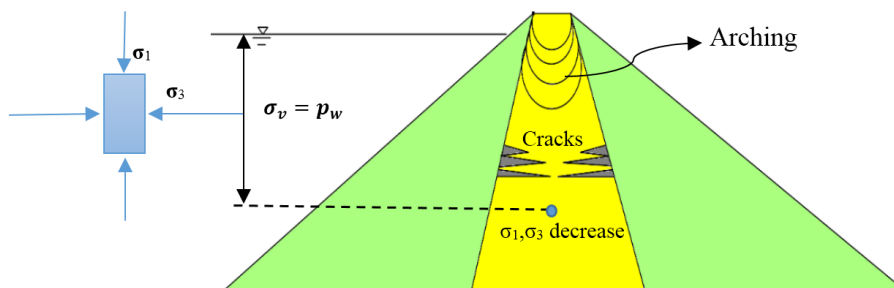


Fig. 3. Hydraulic cracks forming.

In the Eyvashan earth dam and at level 1799m, two piezoelectric immersions are installed at the upstream (EPE229-1) and downstream (EPE229-2) clay core. The variation in the pore water pressure created in the clay core is due to the embankment rise, and in late 2013, with increasing reservoir water level, the pore volume increased, ascending. The last readings reached 649kPa upstream and reached 298kPa downstream, which is shown in Fig. 4. Moreover, in Fig. 5, the ratio of pore water pressure (r_u) to the core height is equal to the excess pore pressure ratio to overpressure. In equation form, the r_u is calculated as:

$$r_u = \frac{u}{\gamma \cdot z} \quad (3)$$

where u is the pore-water pressure, γ is the unit weight of the soil and z is the depth below ground. The denominator (γz) is also known as overburden stress. As can be seen, the maximum value (r_u) for the two piezome-

ters r_{u229-1} and r_{u229-2} is 0.53 and 0.18, respectively. At level 1799m, two pressure cells were set up to equal distances in the upstream (TPC229-1) and downstream (TPC229-2) clay cores, and the arching of the upper reaches of 0.98 was started, and at the last reading of the instrument, this value was 0.53 and reached the bottom of the start and at the last reading to 0.44. Fig. 5.

At level 1812m, two piezometers in the upstream (EPE229-6) and downstream (EPE229-7) clay cores and at 1809m above sea level, three electric piezometers (EPE229-3, 4, 5) in the downstream shell were installed. Piezometers that were installed inside the clay core have experienced a steady trend since the installation, so after the completion of the embankment operation and the beginning of the impounding period, the pore pressure was amortized, and in both of the piezometers upstream and downstream of this pressure was negligible (Figs. 7 and 6).

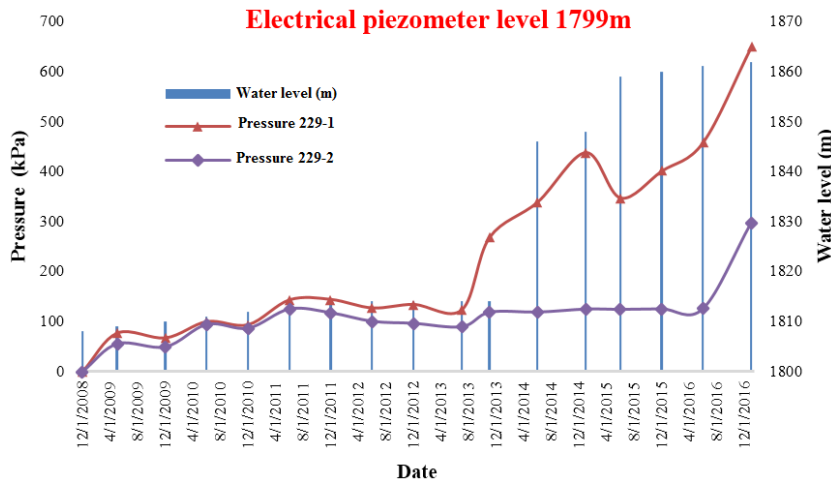


Fig. 4. Pore water pressure changes at piezometer 229-1 and 229-2 (1799m).

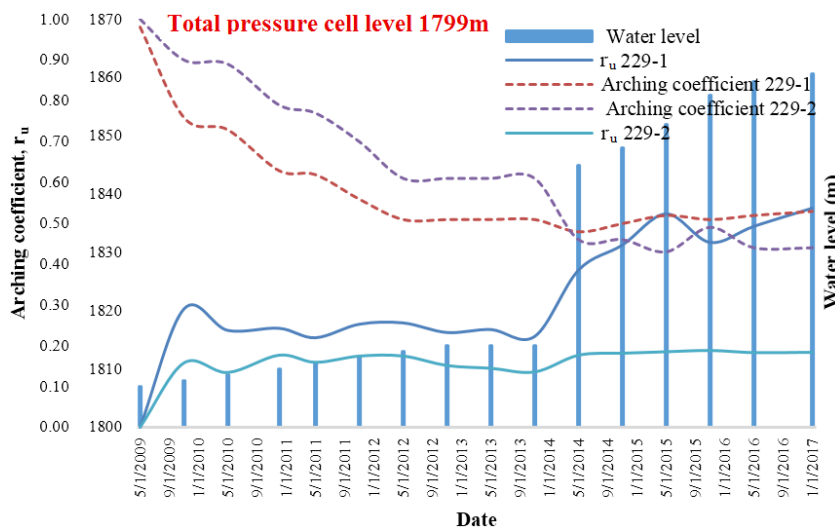


Fig. 5. Water pressure ratio (r_u) and arching coefficient changes at pressure cell 229-1 and 229-2 (1799m).

In the downstream shell, the amount of pore pressure generated was uniform and constant, and the pore pressure created was very small and at zero. The maximum value (r_u) for the piezometer r_u 229-3 and r_u 229-4

was 0.04 and 0.01, respectively. Additionally, the ratio of arching at upstream (TPC229-3) in the last readings provided by the instrumentation was about 0.59 and downstream (TPC229-4) was 0.39 (Fig. 8).

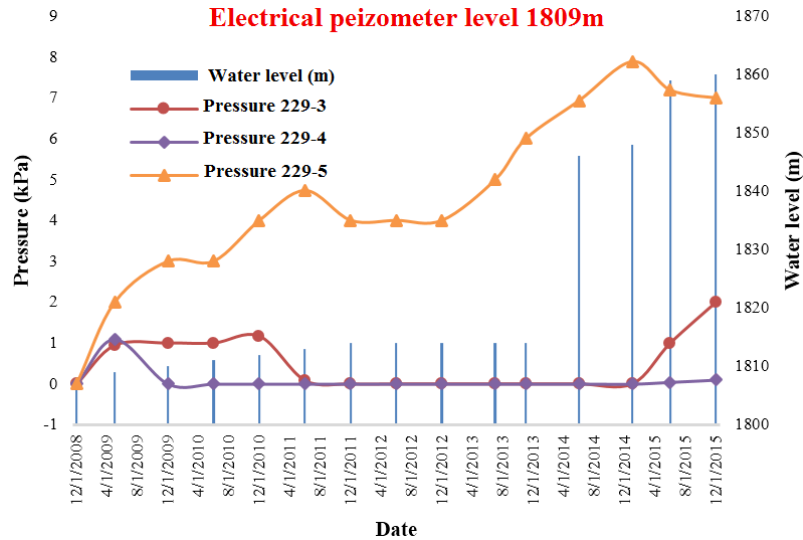


Fig. 6. Pore water pressure changes at piezometer 229-3, 229-4 and 229-5 (1809m).

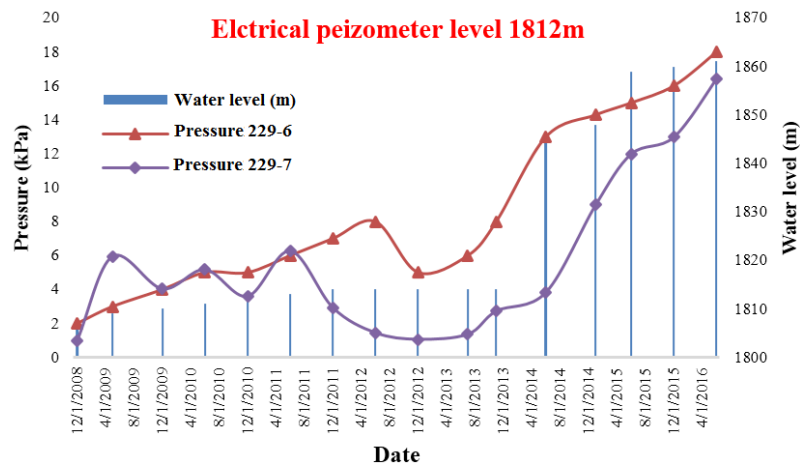


Fig. 7. Pore water pressure changes at piezometer 229-6 and 229-7 (1812m).

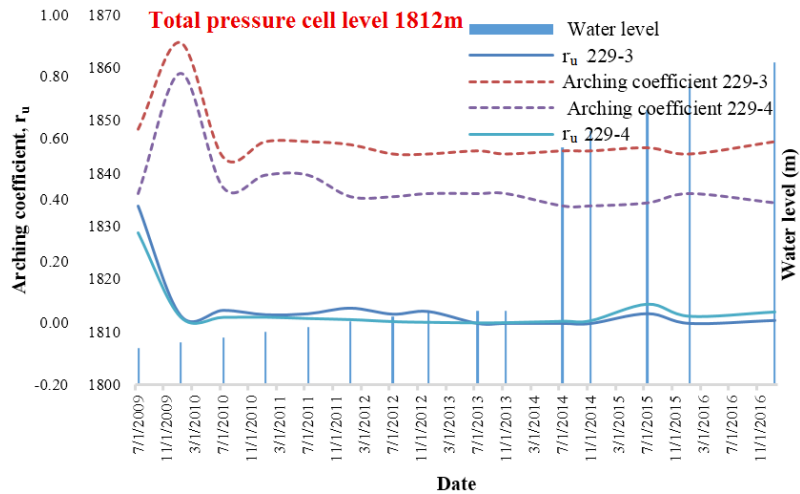


Fig. 8. Water pressure ratio (r_u) and arching coefficient changes at pressure cell 229-3 and 229-4 (1812m).

At level 1825m, two piezometers were located on the upstream and downstream of the clay core and two piezometers in the filter (EPE229-10) and downstream (EPE229-11), a piezometer mounted on the upstream core (EPE229-8) recorded the pressure at 276kPa after the start of intake and at the last reading. Moreover, the bottom-mounted piezoelectric device (EPE229-9) in the last readings showed a pore pressure of about 75kPa but the piezometer mounted in the downstream filter showed the ascending garlic start of the embankment and showed a pressure of about 31kPa in the last reading. The piezometer fitted in the bottom shell at the last reading recorded a piezometer pressure of 138kPa, as shown in Fig. 9. The maximum value (r_u) for the piezometer r_u 229-5 and r_u 229-6 was 0.44 and 0.21, respectively. The arching ratio of level 1825m in the upstream (TPC229-5) ranges from an initial value

of about 0.62 in the last reading of instrumentation. At the downstream (TPC229-6), this ratio ranges from a start to about 0.38. Fig. 10.

At level 1838m, two piezometers of electricity were installed in a clay core and a piezometer in a lane filter. The riser core piezometer (EPE229-12) displayed a 180 kPa pore water pressure and a downstream piezometer of clay core (EPE229-13) with a pressure of 153kPa. The piezometer filter (EPE229-14) showed a very small pore water pressure, which appears to be natural due to the surrounding environment (Fig. 11).

Furthermore, at level 1838m, the arching coefficient in the last reading of instrumentation in the upstream (TPC229-7) was 0.65 and at the end (TPC229-8) was about 0.47. The maximum value (r_u) for the piezometer r_u 229-7 and r_u 229-8 was 0.39 and 0.86, respectively. (Fig. 12).

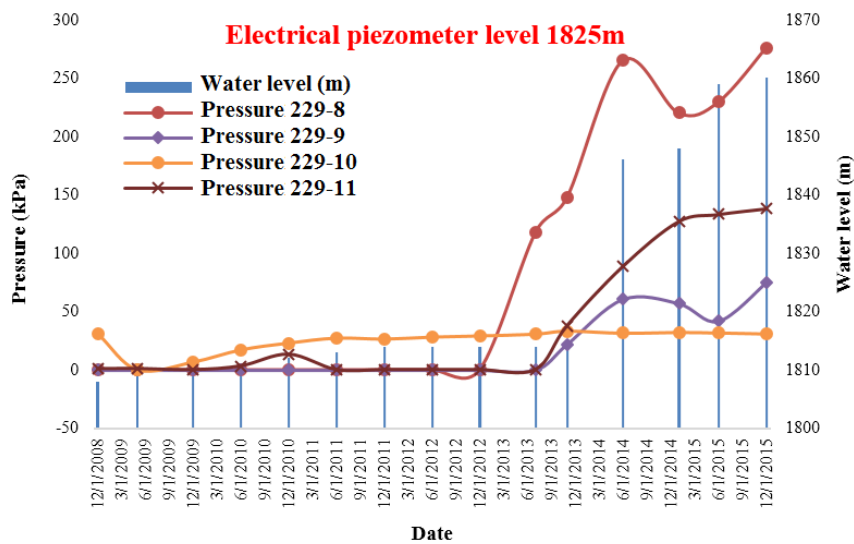


Fig. 9. Pore water pressure changes at piezometer 229-8, 229-9, 229-10 and 229-11 (1825m).

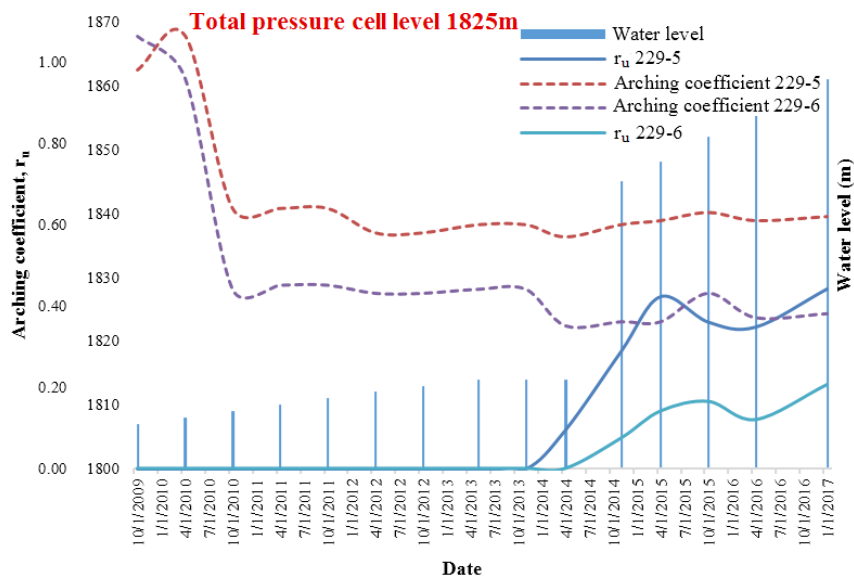


Fig. 10. Water pressure ratio (r_u) and arching coefficient changes at pressure cell 229-5 and 229-6 (1825 m).

The electric piezometer installed at level 1851m has so far shown little and zero pore water pressure, which can be partly due to the dry area around the instrument. The piezometers (EPE229-15, TPC229-9) showed a zero pore water pressure ratio and an arching coefficient of about one at the beginning and at the last reading of the instrument, about 0.51 (Fig. 13).

According to the graphs obtained from the observational data, the highest arching coefficient occurred in the near-filter elements. In fact, the tensions in the middle of the core were more and closer to the filters. Moreover, the rate of arc at higher levels was higher due to less moisture content and lower core width. It is worth noting that the decrease of the arching coefficient with time may be due to the installation of tools and the suppression of pressure within the pressure cells due to various factors, such as the response factor of the soil due to pressure.

3. Results and Discussion

3.1. Geometry and Behavioral Model of Eyvashan Dam Materials

In this research, for the purpose of verifying the data obtained from instrumentation readings, the pore water pressure and arching of the Eyvashan earth dam using the Geostudio modeling software, then the results of the numerical analysis were compared with the results of the observation. The behavior of the body material of the dam and the pill in analyses were considered, the complete elastic-plastic model of Mohr-Coulomb was considered. The Mohr-Coulomb model is one of the simplest soil behavioral models. Since most soil parameters such as dough and elastic soil were present in this model, it was appropriate to model most soil behavioral conditions. The parameters of the materials used in the analysis are presented in Tables 1 and 2.

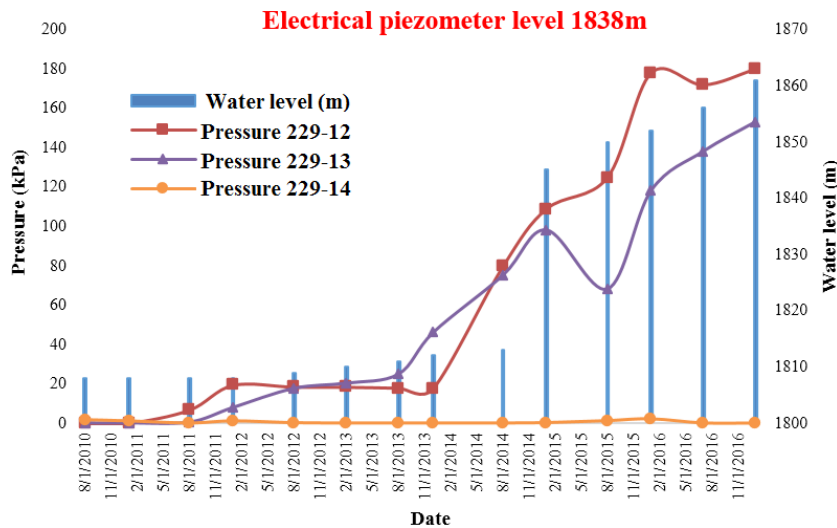


Fig. 11. Pore water pressure changes at piezometer 229-12, 229-13 and 229-14 (1838m).

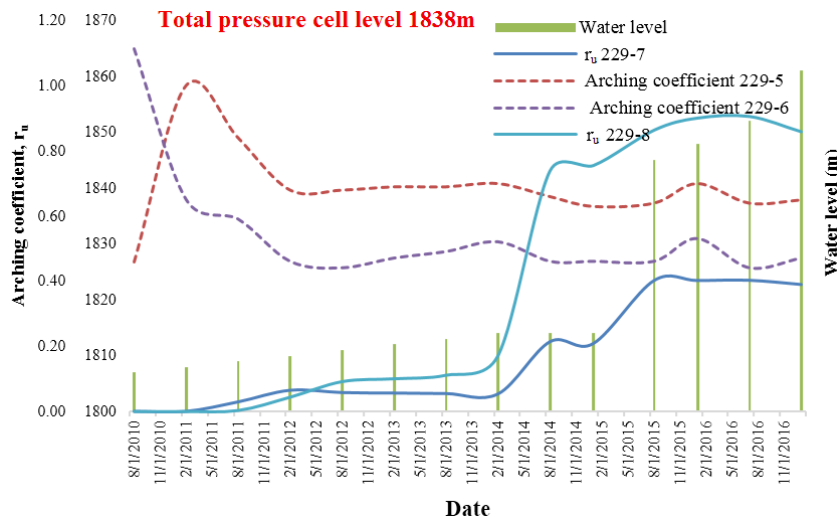


Fig. 12. Water pressure ratio (r_u) and arching coefficient changes at pressure cell 229-7 and 229-8 (1838m)

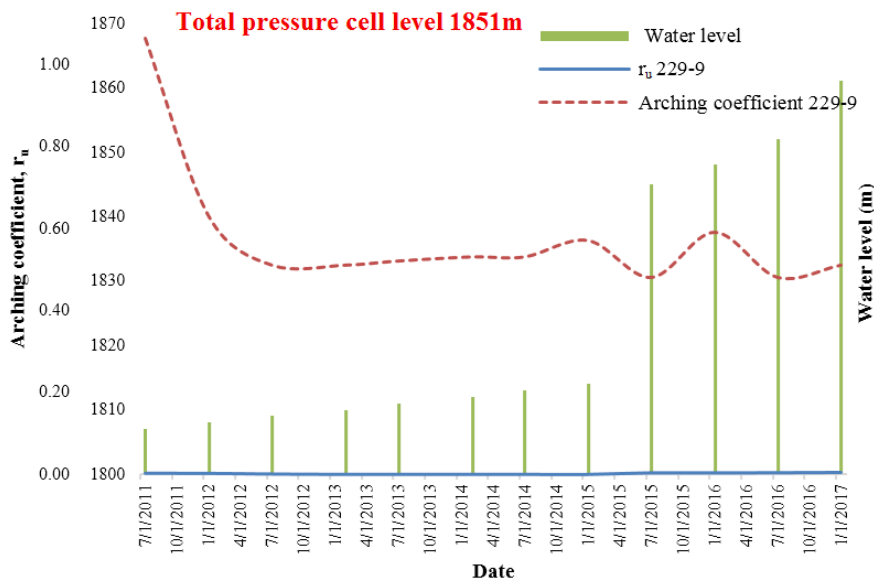


Fig. 13. Water pressure ratio (r_u) and arching coefficient changes at pressure cell 229-9 (1851m).

Table 1

Parameters of materials used in numerical analysis.

Material	Mohr-Coulomb	Type material	E (MPa)	γ_{dry} (kN/m ³)	γ_{wet} (kN/m ³)	γ_{sat} (kN/m ³)	c, c' (kPa)	φ (°)
Core	Mohr-Coulomb	Undrained	35	17.0	20.0	21.0	63.0	11.0
		Drained					28.0	24.0
Shell	Elasto-plastic	70	22.5	23.8	24.5	-	-	-
Filter	Elasto-plastic	45	19.0	21.0	22.0	-	-	-
Drain	Elasto-plastic	55	20.5	22.0	23.0	-	-	-
Alluvium	Elasto-plastic	500	21.5	-	23.2	-	-	-
Foundation	Elasto-plastic	5000	25.5	-	25.0	-	-	-
Cut-off	Elastic	2500	24.0	-	24.0	-	-	-

Table 2

Permeability of various materials of Eyvashan dam.

Materials	Kx (m/sec)	Ky/Kx
Core	2.5×10^{-9}	0.2
Shell	1×10^{-3}	1
Filter	1×10^{-4}	0.5
Drain	2×10^{-2}	1
Alluvial	5×10^{-3}	1
Foundation	1×10^{-9}	1
Cut-off	1×10^{-7}	1

The severity and distribution of pore water pressure, while dependent on the characteristics of consolidation, permeability, and drainage conditions, largely depends on how the work is carried out. Under construction conditions (not impounding), the drain does not exist in dam body, and due to gradual drying, the moisture content of the aggregate is diminished and the vapor water is pressurized only by the weight of the higher layers. Due to the implementation of the layer in the earth dams layer and considering the effect of the density on the properties of the materials, it is clear that in order to obtain accurate results, the earth dam should be modeled in a layer-to-layer manner,

and after applying each layer, the next layer should be a load force on the previous part. If an analysis of a soil dam such as a building or concrete dam is done in one step, tensions and especially deformations will be unrealistic. In this paper, for the modeling of the consolidation settlement and stress-strain formation, the layer-to-layer construction was done in 8 layers and then impounding. The rate of impounding is in such manner that the rise of the reservoir water level at the initial levels is 0.2m/day, and in subsequent steps, with rising water level and expansion of the reservoir, the rate of intake at the last stage has reached 0.1m/day. The duration of absorption up to the normal value is 330 days. After drainage, the analyses continued to increase the excess pore water pressure created by the impounding process and the pore water pressure was nearly stable to reach a stable outflow from the normal value, and subsequent consolidation settlement was determined after drainage. For this purpose, about 2 years after the initial impounding, it is necessary to assume that the water level is constant. In order to examine the pore water pressure of the block in the dam of Eyvashan, the tools installed in

section 229 were selected. The positioning of the body and the foundation, the pore water pressure and the total head contours in the Geostudio model are shown in section 229 of the Eyvashan earth dam (Fig. 14). The pore water pressure at the reservoir floor level is 53.5m, which is equivalent to the reservoir water level (1861.20m). The phreatic line does not show a drop in the upper shell due to the high permeability of the upper crust, and a significant hydraulic gradient is observed in the core, which is evidence of the proper functioning of the core, that is, counteracting the permeability of the flow of water. As can be seen, the parallelism of the pressure lines in the earth's dam is indicative of the continuity of the permafrost current in the body of the earth dam. Overall, the phreatic line in the dam is the boundary between the positive and negative pore pressure, so the points below the phreatic line have positive values of the pore pressure and the points above the line have negative pore pressure values. The cause is a phenomenon of suction in the upper regions. In this research, negative values of pore water pressure with zero are shown. This indicates that the point is at a level above the level of the phreatic line. Moreover, variations in pore water pressure at the core height are plotted at the end of construction relative to the height of the core. As can be seen, the highest pore water pressure occurs at a height of about 6m from the core floor. The results of pore water analysis for numerical analysis and data

analysis using Geostudio software are shown in Table 3.

Fig. 15 compares readings from instrumentation and numerical modeling results for foundation and embankment piezometers. These values are related to the pore water pressure of the body and foundation of the Eyvashan earth dam. In this study, the pore water pressure at zero above the free flow level is considered. Under initial impounding conditions, due to hydrostatic pressure of water, total stresses increase upstream of dam body, because in this case the total stress is obtained from the saturation density of the material. In general, instrument values and numerical analysis have relatively good agreement. The results of arching numerical analysis and instrument readings are shown in Table 4.

In Fig. 16, the total vertical stress contours of section 229 of the Eyvashan dam are shown and it is observed that the total stress values in the upstream and downstream areas are approximately parallel to the embankment surface and the curved position has changed in the central region of dam (clay core). In each horizontal plane, the maximum amount of stress in the transitional layer is upstream and downstream of dam (filter and drain) and decreases to the slope of the crust. In fact, the decrease in stress in the clay core is due to the transfer of the charge from the core to the faces and the occurrence of the arching phenomenon.

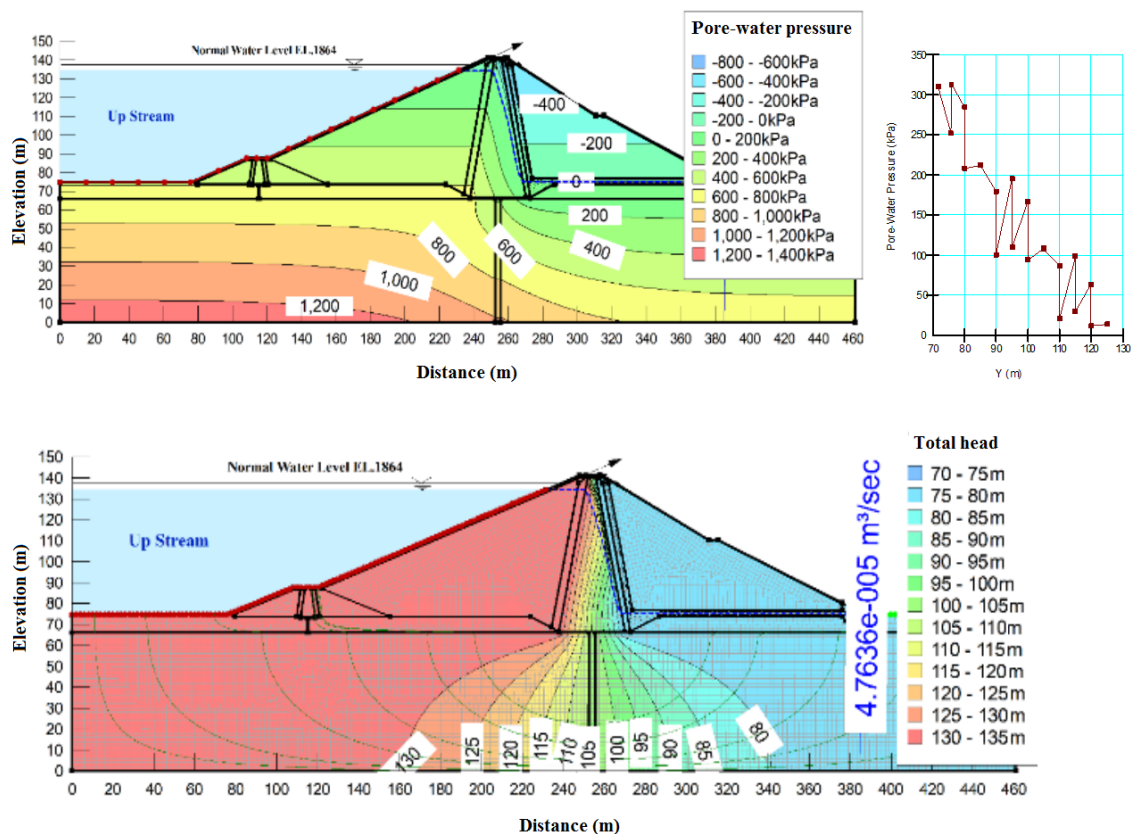


Fig. 14. Flow lines and total head contours in Geostudio software.

Table 3

Measured and predicted values of pore water pressure for electrical piezometer installed in core of Eyvashan dam (section 229).

Piezometer	Level (masl)	Measured value of the pore water head (m)	Estimated values of the pore water head (m) Geostudio
EPE-1	1806.32	46.75	48.4
EPE-2	1806.30	12.82	7.1
EPE-3	1809.20	1.4	0
EPE-4	1809.25	0.5	0
EPE-5	1809.26	0.43	0
EPE-6	1812.20	0.37	2.6
EPE-7	1812.12	1.58	1.7
EPE-8	1825.36	28.15	26.7
EPE-9	1825.27	7.61	6.1
EPE-10	1825.29	3.15	4.19
EPE-11	1825.22	14.12	10.78
EPE-12	1838.29	18.11	20.6
EPE-13	1838.41	27.12	18.7
EPE-14	1838.51	0.1	0
EPE-15	1851.35	0.1	2.6
EPF-1	1778.2	71.26	74.51
EPF-2	1778.2	59.09	64.94
EPF-3	1778.2	66.92	69.46
EPF-4	1788.2	30.6	27.64
EPF-5	1788.2	13.42	8.54
EPF-6	1788.2	14.7	13.28

Table 4

Measured and predicted coefficient of arching for pressure cell installed in core of Eyvashan dam (section 229).

Piezometer	Elevation (m)	Arching coefficient (Before impounding)		Arching coefficient (After impounding)	
		Instrument	Geostudio	Instrument	Geostudio
TPC-1	1806.40	0.76	0.73	0.60	0.62
TPC-2	1806.36	0.70	0.72	0.54	0.58
TPC-3	1812.24	0.71	0.71	0.63	0.63
TPC-4	1812.16	0.58	0.61	0.44	0.54
TPC-5	1825.45	0.73	0.72	0.62	0.65
TPC-6	1825.39	0.61	0.69	0.50	0.59
TPC-7	1838.35	0.83	0.82	0.66	0.68
TPC-8	1838.35	0.68	0.78	0.53	0.65
TPC-9	1851.36	0.63	0.68	0.56	0.59

Analyses show that the vertical stresses and the principal stresses are maximally reduced at the core, shell junctions, undergo abrupt changes. This drop represents the occurrence of the phenomenon of arching. For better comparison, the values of arching percentage were modeled before and after the impounding and compared with the results of instrumentation at different levels (Figs. 17 and 18). In Fig. 19, the ratio of the arching of the core $\left(\frac{\sigma_v}{\gamma \cdot h}\right)$ to the overhead stress ratio at the point of interest is plotted to the height of the core, indicating that the highest arching (arching ratio) is equal to 46% and at $\frac{1}{3}$ of the core height Floors have occurred. In fact, the critical arching is 0.44, which is as normal [15].

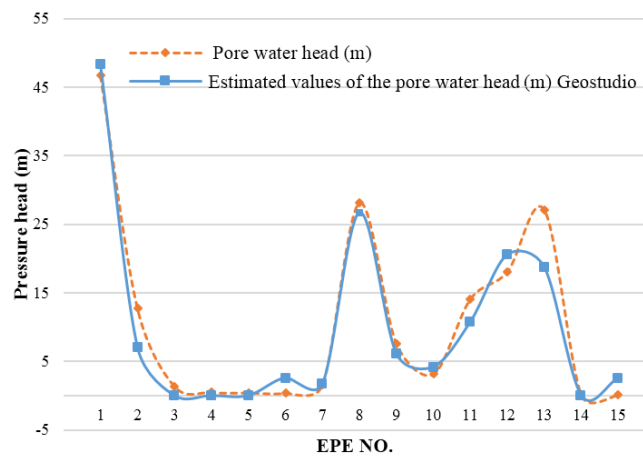


Fig. 15. Comparison of instrumentation and numerical analysis of pore water head, electric piezometers Embankment.

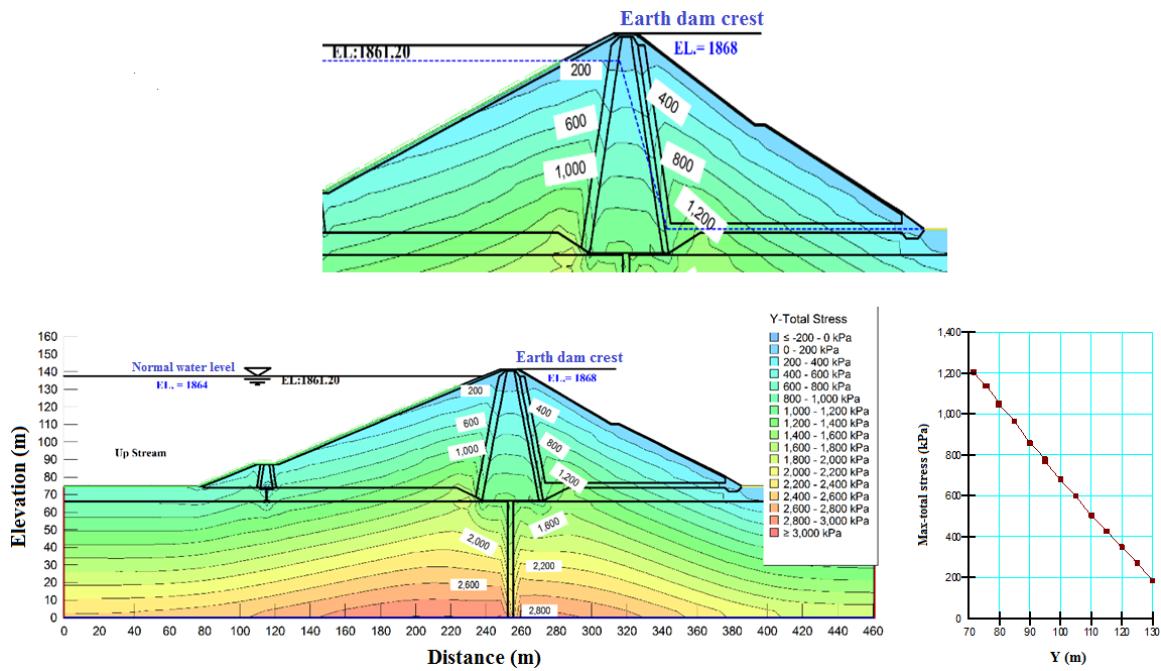


Fig. 16. Total stress contours and stress-strain analysis after impounding.

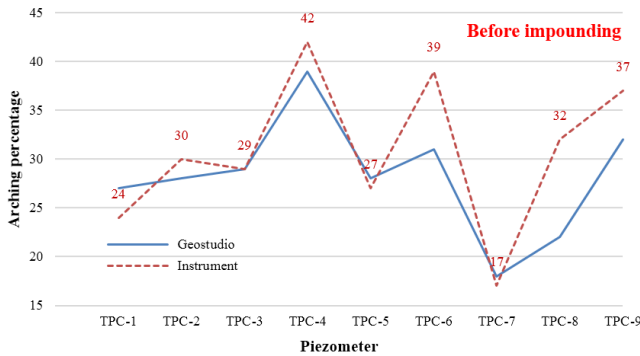


Fig. 17. Comparing the results of the instruments and numerical modeling in relation to the percentage of arching (before initial impounding).

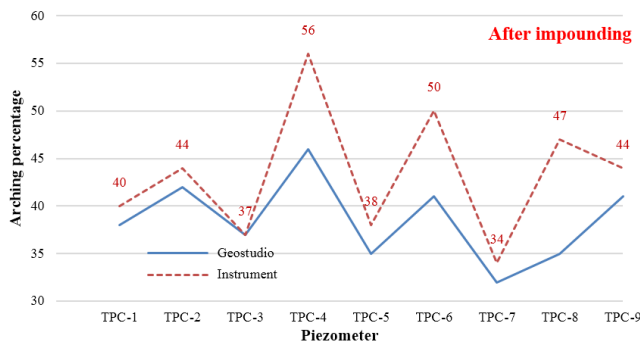


Fig. 18. Comparing the results of the instruments and numerical modeling in relation to the percentage of arching (after initial impounding).

In Figs. 17 and 18, the amount of arching after impounding the dam increases. Furthermore, the arching percentage of the barometers in the core is different so that the downstream of the clay core is higher than the upstream. These changes are in the vicinity of

lower pressure gauges with the filter area and drainage underlying cluster, while there is a lower width filter area on the upstream core. It is worth noting that a filter area with a width of 2.5m is located at the upstream core, and two filter and drain regions both have a width of 3m at the downstream of the core. Additionally, the percentage change of the equilibrium points after initial impounding significantly increased compared to the construction period, and this increase could be due to the damping of dam and the state of saturation of the core and the body above the phreatic line. Of course, the results show that the damping of the dam has the greatest effect on the high levels, while at higher heights it is about 100 percent and at lower levels, about 50 percent is increased by arching before initial impounding, which can be due to lower core width at higher levels. However, the highest percentage of arching was initially constructed from the beginning to the end of the impounding stage in the lower parts of the core. The difference between the results of the instrumentation arching and the numerical analysis results can be due to the performance issues, the type of materials used, the percentage of congestion used, drained upstream and downstream of dam core, which may also be related to software deficiencies. In Fig. 20, total and effective vertical stress variations, variations in pore water pressure and γh are plotted relative to the height of the core. The loss of effective stresses and absolute vertigo relative to γh is due to the arching phenomenon. The effective vertical stress drop is far greater than the total vertical stress because in this case the additional pore water pressure created during the construction process also decreases the total stress. The effective and total horizontal stress distri-

bution at the dam height at the end of the dam construction is shown in Fig. 21.

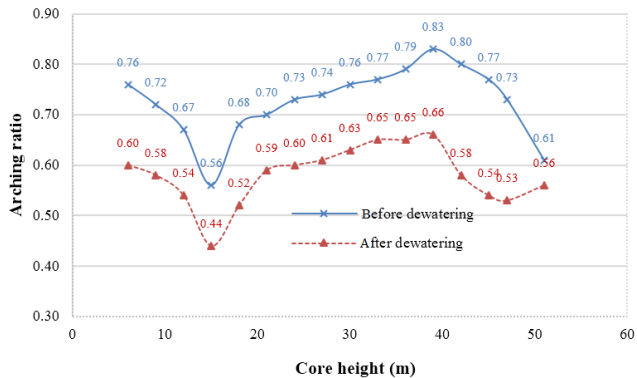


Fig. 19. Changes in the arching coefficient of core height.

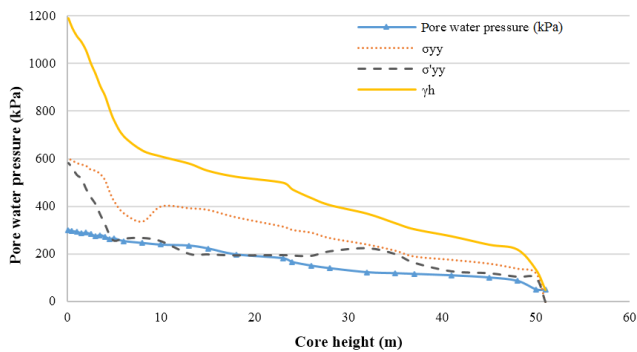


Fig. 20. Total and effective vertical stress variations, excess water pressure and γh at the core height (core center).

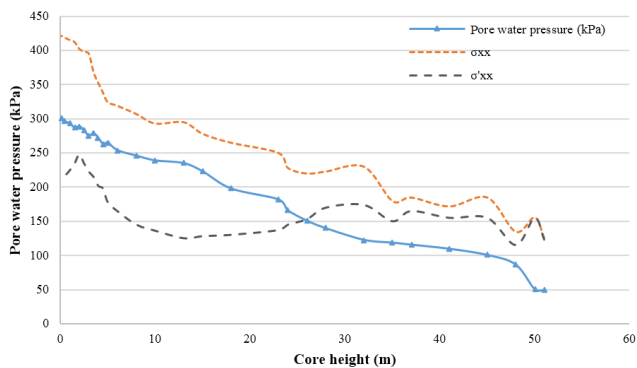


Fig. 21. Total and effective horizontal stress variations, excess water pressure and γh at the core height (core center).

As can be seen, the effective horizontal stress at any point in the core is not be equal to zero.

3.2. Hydraulic Failure

The hydraulic fracture phenomenon means cracking due to the water pressure. This phenomenon is likely to occur after reservoir impounding and pressure application in the dam sealing element (central clay core) at points where the water pressure from the main stress

is minimized. In order to investigate this phenomenon, it is necessary to minimize the pressure of water with the main stress in all points of damping element. Since in the first impounding, especially when the velocity is high, there is no possibility of water penetration in the core; generally, critical points are located at the upper end of the core; these are local points where there is a potential for water penetration. It is therefore conservative to suppose that there is complete hydrostatic pressure behind the clay core (the first element of the clay core in the upstream). If these elements can withstand the pressure of the water, it is virtually upstream and downstream of the core to be cut-off and hydraulic leaving will not occur, so safety will be provided. To investigate this phenomenon, the horizontal and vertical stresses in the upper and lower elements of the core are plotted in relation to the height of the core in Fig. 22, as well as the variations in pore water pressure against the height of the core of dam in the same diagram. As indicated, vertical and horizontal tensions are at most and at least at all levels more than water pressure, therefore hydraulic fractures do not occur at the core of this dam. However, due to the high thickness of the core in the Eyvashan dam, there is little concern about the hydraulic fracture phenomenon.

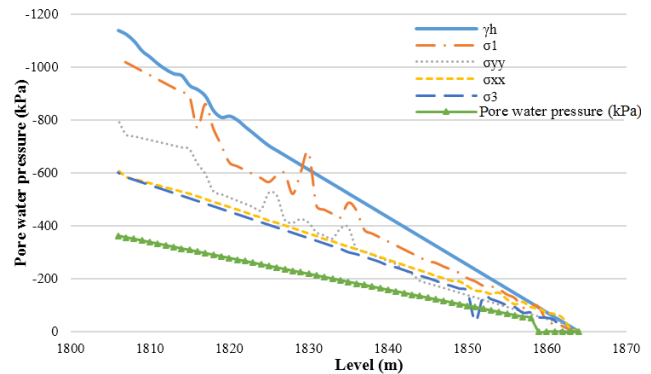


Fig. 22. Evaluation of hydraulic failure in the core.

4. Conclusions

Static analysis of the Stress-Strain of the Eyvashan dam during the construction and initial impounding stage was such that there is no problem in terms of stability for the dam. Analyses showed that the vertical stresses and maximum stresses in the range of core and shell attachment fall and have a sudden change. This drop represents the occurrence of the arching phenomenon. The highest percentage of arching (the lowest arching ratio) was 46% and at $\frac{1}{3}$ of the height of the core of the floor. The arching ratio was 0.44, which is as normal. Moreover, the values of pore pressure and (r_u) were acceptable. Hydraulic fractures did not occur even if the arching phenomenon came to the foregoing point in the dam, and because of the high thickness

of the core in the Eyvashan dam, there was little concern about the hydraulic fracture phenomenon. The results of the analysis confirm the proper behavior of dam body against water pressure during construction and at the impounding stage. Tensions were acceptable and the stability of dam was based on strain-strain analyses. In general, the results of the analysis confirm the proper behavior of dam body against different static loading conditions.

References

- [1] B. Lofquist, Discussion of cracking in dams, In: Proceedings 5th ICOLD Congress Paris, Vol. III, (1957) 21-22.
- [2] J.L. Sherard, Hydraulic fracturing in embankment dam, *J. Geotech. Eng.*, 112(10) (1986) 905-927.
- [3] M. Maksimovic, Optimal Position of Central Clay Core of Rock-Fill Dam with Respect to Arching and Hydraulic Fracture, *International Congress on Large Dam*, (1973) 789-800.
- [4] F.H. Kulhawy, T.M. Gurtowski, load transfer and hydraulic fracturing in Zoned Dams, *J. Geotech. Eng. Div.*, 102(9) (1976) 963-967.
- [5] J.J. Wang, J.G. Zhu, H. Mroueh, C.F. Chiu, Hydraulic fracturing of rock-fill dam, *J. Multiphase*, 1(2) (2007) 199-219.
- [6] K. Soga, M.Y.A. Ng, K. Gafar, Soil Fractures in Grouting. In: Barla, G., Barla, M. (Eds.), *Proc. 11th International Conference of the International Association of Computer Methods and Advances in Geomechanics, Prediction, Analysis and Design in Geomechanical Applications*. Torino, Italy, (2005).
- [7] H. Satoh, Y. Yamaguchi, Laboratory hydraulic fracturing tests for core materials using large size hollow cylindrical specimens, *The 1st International Symposium on Rock-fill Dams*, (2009).
- [8] M.R. Mansoojian, M.R. Esmaeili, A. Kohzadian, Investigation of Hydraulic Failure in earth Dams and Structures Using SIGMA/W Software, 5th National Conference on Irrigation and Drainage Networks Management and Third Iranian National Irrigation and Drainage Congress, (2017).
- [9] A.R. Molavi, A.P. Parvishi, Investigation of hydraulic failure of earth dam under the impact of near-earthquake, 5th National Conference on Applied Research in Civil Engineering, Urban Architecture and Management, Tehran, (2017).
- [10] M. Rezapur Tabari, M. Hashempour, Investigation of Parameters Effective on Hydraulic Failure of Dam, Second National Conference on Hydrology, Tehran, (2017).
- [11] B. Abbasi, K. Esmaeili, J. Abrishami, Simulation of the hydraulic fracture failure of dam with rapid flood entry into the reservoir, *J. Water Soil*, 24(1) (2010) 75-83.
- [12] S.A. Khamesi, A.S. Mirghasemi, Investigation of hydraulic failure in earth dams, *J. Civi. Surv. Eng.*, 44(2) (2010) 181-191.
- [13] M. Salari, A. Akhtarpour, A. Ekrami Fard, Occurrence of hydraulic fracturing in inclined clay core of a high rockfill dam, located in narrow valley, *Modares Civ. Eng. J.*, 17(5) (2017) 109-122.
- [14] A. Asakareh, M. Ahang, Numerical analysis of arching phenomenon at core of baft zoned embankment dam, *Kerman, Modares Civ. Eng. J.*, 17(5) (2017) 161-168.
- [15] A. Ghanbari, *Principles of Earth Dam Engineering*, Kharazmi University Publication, (2014).